FACULTY
OF SCIENCE

Self-bound droplets in quasi two-dimensional dipole-dipole interacting Bose-Einstein condensates

David Boholm

Thesis submitted for the degree of Bachelor of Science
Project duration: 2 months, 15 hp

Supervised by Stephanie Reimann

Department of Physics
Division of Mathematical Physics
December 2018

Abstract

Ultra-dilute self bound droplets in Bose-Einstein condensates have been of great interest since their first prediction in 2015. The self-bound nature of these bosonic gases combined with their extremely low densities make them a prime target of investigation for both experimentalists and theoreticians. In this thesis work dipole-dipole interacting gases are simulated using the Gross-Pitaevskii equation applying a fourth order, split-operator imaginary time method in two dimensions. First, the systems are studied at collapse for dipoles aligned with a magnetic field that tilts the dipoles in the two-dimensional plane. For some angles the dipole interaction becomes partly attractive which can lead to the collapse of the mean field solution. However, quantum fluctuations can stabilize the gas. Introducing the so-called Lee-Huang-Yang (LHY) correction, the system can be stabilized and self-bound droplets may form. Here, we investigate this stabilization for a quasi two-dimensional set-up.

Popular science

Ultra-cold droplets intrigue physicists

A hot topic within ultra-cold atom physics has been the recent discovery of droplets formed out of Bose-Einstein condensates, a specific form of a super cold and very dilute gas. The condensate is however very different from any gas encountered in everyday life. A normal gas can be thought of as atoms or molecules moving around in all directions. If you cool this gas, all the particles move slower until they either form a liquid or freeze and become a solid.

This is not the case for the Bose-Einstein condensate. Instead they spread through space due to quantum mechanics and together they form one entity. This entity, the so called condensate, behaves like no classical gas, as it is mainly governed by quantum mechanics and not by the random chance of a lot of small particles moving about.

To add to this strangeness, droplets now seem to form out of these condensates. The existence of these droplets was quite a surprise. Among experimentalists working with creating Bose-Einstein condensates the expected result was a collapse of the system if forces pushing the condensate together won against the forces pushing it apart. However, experimentalists revealed that some other internal force stabilized drops inside the condensate. Not only that, this force seemed to be able to create drops that could exist outside a "trap", which usually is a number of lasers and magnets that keep the condensate together. Some droplets could not be formed without a trap, but instead formed crystal structures, a very intriguing result.

This has led to an excited mood within the field of cold atom physics. But what to expect from this anti-collapse force, mainly being described as quantum fluctuations, and the droplets it creates needs further study to find out. In this thesis work we simulate the anti-collapse force and possible droplet systems solving the underlying quantum-mechanical many-particle equations numerically.

One system of interest is the very thin disc of condensate, or a quasi two-dimensional condensate. This system is excellent for rotating the condensate in. Why? Imagine having a piece of pizza dough that in this case represents a condensate. If you spin this dough as a skilled pizza maker does, the pizza will become flat due to rotational forces. The same goes for the condensate. As you rotate it it will become flat anyways and therefore having a model where our very cold gas is already flat makes it easier to simulate rotating systems.

But before you start rotating your drops, you have to find the drops. And to find the drops you have to study the forces pushing the condensate together and the forces pushing it apart. Therefore we presently aim at studying possible droplet formation in these pizza crust shaped condensates, to make way for the study of rotational excitations. Initial results show some promise that droplets can be found in these quasi two-dimensional systems.

Acknowledgements

I would like to thank my supervisor, Stephanie Reimann, for all the support, help and enthusiasm during this Bachelor Thesis work. I would also like to thank Philipp Stürmer for the help and the interesting discussions during this period. To Jacob Taxén, Pernilla Helmer, Gunnar Eriksson, Mikael Nilsson Tengstrand, Josef Josefi and Jakob Bengtsson who read and corrected my report I give special thanks. Last but not least I would like to thank Irene Geijselaers and Jill Wiberg who always have a couch for me when I am feeling down and sad. Thank you!

List of Acronyms and Abbreviations

BEC	Bose-Einstein condensate
GPe	Gross-Pitaevskii equation
2D	Two-dimensional

Contents

Chapter 1 | Introduction

The study of Bose-Einstein condensation has given us access to new fascinating physical systems where quantum mechanical laws can be studied up close. Much effort has been put into realizing and studying these systems during the past years [1, 2]. A recent and interesting development within the field of research is droplet formation in Bose-Einstein condensates [4, 5, 6]. These droplets are seemingly meta-stable outside their trap-based experimental set-ups. The reason for this unexpected stability lies in quantum fluctuations that until now have been disregarded as higher terms that can be omitted from leading mean-field theories. These droplets share some physical characteristics. Most importantly all droplets have several competing interactions, either dipole-dipole interactions or inter-species forces, competing with a contact interaction. The dipole-dipole interaction force has both repulsive and attractive regions that can, if tuned correctly, overcome the repulsive contact interaction. In the most common mean field descriptions this leads to an unphysical collapse of the condensate. However, this collapse is stopped by quantum fluctuations, often described by the Lee-Huang-Yang correction [3]. With this correction the collapse instead becomes droplet formation. The existence of these stable, self-bound quantum systems has opened a new horizon for the physics of ultra-cold quantum gases.

So far, the main area of investigation for dipolar condensates has been droplet crystallization where the droplets are not self-bound but are instead confined. In a trapping potential these droplets form crystal structure [4]. In two-component gases, the study of self-bound droplets has been a main interest, where the theoretical proposal [5] and the experimental realization [6] were only two years apart. The LHY term for dipolar gases has been theoretically derived by Lima and Pelster [7] whose work has been used to explain the droplet crystallization [8]. Their main area of study was however the regime of three-dimensional condensates. What has yet to be thoroughly investigated are low-dimensional dipolar Bose gases where the contact interaction is tuned such that the dipole-dipole interaction, according to first order mean field theories, would cause a collapse of the condensate. The LHY correction term might have a large impact in such a system, with one possibility being that self-bound droplets can be found. Both quasi two-dimensional and exact two-dimensional condensates are relatively unexplored compared to three-dimensional systems.

In this thesis work a quasi two-dimensional (quasi 2D) dipole-dipole interacting Bose gas has been studied in the regime where the dipolar interaction overcomes the contact interaction. For this task a fourth order, split-operator, imaginary time propagation method [9] has been used to solve the Gross-Pitaevskii equation. A LHY term was introduced into this framework to see how it affected the condensate shape and energy and whether a collapse of the wave function was hindered. If collapse was hindered the wave function from that calculation was used as initial state in a calculation where the external trap was removed. This to see if the state was self bound. Several different dipole interaction strengths were tested with varying contact interaction strengths. Before discussing our main findings, this thesis begins with a brief review of the subject of Bose-Einstein condensates, their theoretical simulation and droplet formation in Bose gases.

Chapter 2 | Bose-Einstein condensation in theory and experiments

Due to the possibility for bosons to inhabit the same quantum state, systems consisting of very cold bosons behave as if they were one quantum mechanical object. These Bose-Einstein condensates (BEC:s) were proposed in 1925 [10] but were not experimentally realized until 1995 [11]. In the mean time, the theories of the condensate have given insight into fundamental properties of both super-fluids and super-conductors [1].

In this chapter we will provide a brief overview of the BEC, concerning experiments and theory. In section 2.1 we will discuss the general phenomenon of Bose-Einstein condensation, looking at its field-like properties and introduce the contact interaction. Then, we discuss the Gross-Pitaevskii equation in section 2.2. In section 2.3 we look at the realization of BEC:s in extremely dilute alkali gases and what results came from studying them.

2.1 The Bose-Einstein condensate

Bose-Einstein condensation was proposed in 1925 by Albert Einstein in a paper elaborating the ideas of Satyendra Bose concerning particles with integer spin [2]. These particles, called bosons, are not confined to one particle per quantum state, as prescribed by the Pauli principle for fermions, but can share a single-particle state with each other. In the case of a gas of bosons the particle distribution over states is governed by the Bose distribution

$$f^0(\epsilon_\upsilon) = \frac{1}{e^{(\epsilon_\upsilon - \mu)/kT} - 1} \tag{2.1}$$

where f^0 is the occupation number, ϵ_υ is the energy of the state, μ is the chemical potential (as the particle number is constant), k is the Boltzmann constant and T is the temperature. μ varies with temperature and the number of particles [1]. The chemical potential is however limited in how much it can vary as the lowest energy level, ϵ_{min}, cannot be surpassed due to the distribution function then turning negative, which is an unphysical result. Instead, when very low temperatures are reached we find that the particle number decreases if we integrate the distribution over all energy levels. The particles that have seemingly vanished have all fallen down in the lowest energy state where they form a peak in the distribution that is not included in the integral. These particles have condensed into a BEC and the gas now has a condensate fraction, given by

$$N_0 = N\Big(1 - \Big[\frac{T}{T_c}\Big]^3\Big) \tag{2.2}$$

in the case of a three-dimensional harmonic trap. Here N is the number of particles, T is the temperature and T_c is the transition temperature, the temperature at which a condensate fraction first starts appearing [1].

We now turn to the description of this condensate as described in Ref. [2]. As the gas descends into condensate form, the one-body density matrix can be described by

$$n^1(r,r') = N_0\phi_0^*(r)\phi_0(r') + \sum_{i\neq 0} n_i\phi_i^*(r)\phi_i(r') \tag{2.3}$$

where N_0 is the number of particles in the single particle ground state $\phi_0(r)$ and the sum describes the contribution from higher single particle states, ϕ_i where $i \neq 0$. This is especially convenient when N_0 is of the order N and n_i is of order one. This can in turn be used to go from a particle to a field description. Using Eq. (2.3) one can rewrite the second quantization field operator $\hat{\Psi}(r)$ as a sum of creation operators, $\hat{a}_i$, weighted by individual particle wave functions, $\phi_i(r)$,

$$\hat{\Psi}(r) = \phi_0(r)\hat{a}_0 + \sum_{i\neq 0}\phi_i(r)\hat{a}_i \tag{2.4}$$

where one starts by separating out the condensate state. Now, for the case where N_0 is close to N one can use the Bogoliubov approximation where $\hat{a}_0 = \sqrt{N_0}$ [2]. Here one uses the fact that $\langle a_0^\dagger a_0\rangle \approx N_0$ and the commutation relation $[a_0^\dagger, a_0]$ being one, which means that one can approximate that the two operators commute. This turns the separate condensate state operator term in Eq. (2.4) into a field, turning the field operator in Eq. (2.4) into

$$\hat{\Psi}(r) = \sqrt{N_0}\phi_0(r) + \delta\hat{\Psi}(r). \tag{2.5}$$

When only the condensate state is occupied, the gas can be seen as a classical field, much like photons for some limits can be seen as electro-magnetic fields [2].

Before moving on to the mean field theories of BEC:s, we will quickly look through the energies involved in the condensate. In the case of the individual particle in a non-interacting ideal gas the Hamiltonian is simply

$$\hat{H} = -\frac{\hbar^2}{2m}\nabla^2 + U(r). \tag{2.6}$$

In this thesis, however, the main topic is the weakly interacting Bose gas, where there is a contribution to energy from the interactions between the particles. To avoid high order interactions with three or more particles interacting one assumes a dilute gas. The diluteness, combined with the low temperature, also leads to the s-wave scattering length a_s being the one governing variable when it comes to interactions. Using the second quantization operator, one can set up a Hamiltonian for the entire system with contact interaction [2],

$$\begin{aligned}\hat{H} = &-\frac{\hbar^2}{2m}\int dr\nabla\hat{\Psi}^\dagger(r,t)\nabla\hat{\Psi}(r,t) + \int dr\hat{\Psi}^\dagger(r,t)U(r)\hat{\Psi}(t) \\ &+\frac{1}{2}\int \hat{\Psi}^\dagger(r,t)\hat{\Psi}^{\dagger\prime}(r',t)V_{\mathrm{Con}}(r'-r)\hat{\Psi}(r',t)\hat{\Psi}'(r,t)dr'dr\end{aligned} \tag{2.7}$$

where $V_{\mathrm{Con}}(r'-r)$ is the contact interaction potential and $U(r)$ is an external potential. If one Fourier transforms the system into momentum space and plugs in the right hand side of Eq. (2.4) in Eq. (2.7) one obtains

$$\hat{H} = \sum_p \frac{\hat{p}^2}{2m}\hat{a}_p^\dagger\hat{a}_p + U + \frac{1}{2V}\sum_{p_1,p_2,q} {}^{\mathrm{Con}}V_q\hat{a}_{p_1+q}^\dagger\hat{a}_{p_2-q}^\dagger\hat{a}_{p_1}\hat{a}_{p_2} \tag{2.8}$$

where U is the external potential in momentum space, V is the volume of the system, ${}^{\text{Con}}V_q$ is the contact interaction with q being the transferred momentum in a certain interaction and $\hat{a}_p/\hat{a}_p^\dagger$ being the momentum-space annihilation/creation operators.

Now we look at at all the possible interactions between two particles with momenta p_1, p_2 and with the momentum exchange q. In the case of a condensate at zero temperature all particles will be in the $p_1 = p_2 = q = 0$ state. This means that by using the Bogoliubov approximation we obtain the following expression for the contact interaction energy:

$$\hat{H}_{\text{Con}} = \frac{Nn\ {}^{\text{Con}}V_0}{2} \tag{2.9}$$

where n is the density of the system. The inter-particle potential ${}^{\text{Con}}V_0$ is usually denoted as the interaction strength g and can, for three dimensions, be shown to be

$${}^{\text{Con}}V_0 = g = \frac{4\pi\hbar^2 a_s}{m} \tag{2.10}$$

where a_s is the s-wave scattering length and m is the mass of the individual bosons [2].

The s-wave scattering length is a measure connected to the cross-section and therefore to the probability of a particle interaction. If the interaction is weak we can approximate the interacting particles wave function as a free particle wave. This is called the lowest order Born approximation and gives us the following scattering length relation to the differential cross-section as

$$\frac{d\sigma}{d\Omega} = |a_s|^2 \tag{2.11}$$

where $d\sigma$ is the the number of particles per unit area and $d\Omega$ is the differential solid-angle element [12]. For higher orders of Born approximations we create the transition operator T, defined as

$$V\,|\psi\rangle = T\,|\phi\rangle \tag{2.12}$$

where V is the interaction potential, $|\psi\rangle$ is the scattered particle state and ϕ is a free particle state. We now use the Lippmann-Schwinger equation to approximate the scattered particle state, $|\psi\rangle$, as

$$|\psi\rangle = |\phi\rangle + V\frac{1}{E - H_0 - i\epsilon}\,|\psi\rangle \tag{2.13}$$

where E is the energy of the interaction, H_0 is the free particle Hamiltonian and ϵ is a very small variable creating ań imaginary pole making the Lippmann-Schwinger equation possible to solve when $E - H_0 = 0$. By multiplying the Lippmann-Schwinger equation with V we find T to be

$$T\,|\phi\rangle = V\,|\phi\rangle + V\frac{1}{E - H_0 - i\epsilon}T\,|\phi\rangle \tag{2.14}$$

If one uses this transition operator and calculates the scattering length a one gets

$$a = \frac{2m_r}{2\pi\hbar^2}(2\pi)^2\,\langle k'|\,T\,|k\rangle \tag{2.15}$$

where m_r is the reduced mass (in the case of equal mass between the interacting particles $m_r = m/2$), $|k'\rangle, |k\rangle$ are the incoming/outgoing momentum states and T is

$$T = V + V\frac{1}{E - H_0 - i\epsilon}\left[V + V\frac{1}{E - H_0 - i\epsilon}\big(V + V\frac{1}{E - H_0 - i\epsilon}...\big)\right] \tag{2.16}$$

The sum described by the combination of Eq. (2.15) and Eq. (2.16) is called the Born series [12]. In most of this work we only use the first order term of the sum, V and get the s-wave scattering length in Eq. (2.10), if we set $k' = k = 0$. Higher order Born series terms will make a small appearance later as we move onto the effect of quantum fluctuations for the contact interaction energy. But for the moment, we only look at the perfectly condensed BEC that introduces us to a more simplified version of the weakly interacting gas energy. When we later encounter effects by quantum fluctuations we will have to revisit this theory and do a more stringent derivation of the two-particle interaction. For now, it is however sufficient to only look at the basic contact interaction in order to introduce the mean-field equation whose solutions will be the main results of this thesis work: the Gross-Pitaevskii equation.

2.2 Gross-Pitaevskii equation in three and two dimensions

The Gross-Pitaevskii equation (GPe) was derived individually by Gross and Pitaevskii in 1961 in the quest to find a mean-field equation of motion for the condensate as a whole [2]. To obtain this we first find the time derivative for the creation/annihilation operator $\hat{\Psi}(r,t)/\hat{\Psi}^\dagger(r,t)$ for which we have the commutation relations

$$[\hat{\Psi}(r,t), \hat{\Psi}^\dagger(r',t)] = \delta(r-r') \tag{2.17}$$

$$[\hat{\Psi}(r,t), \hat{\Psi}(r',t)] = 0 \tag{2.18}$$

In the Heisenberg representation the time derivative for $\hat{\Psi}$ is given by

$$i\hbar\frac{\partial\hat{\Psi}(r,t)}{\partial t} = [\hat{\Psi}(r,t), \hat{H}]. \tag{2.19}$$

Inserting the Hamiltonian in Eq. (2.7) into Eq. (2.19) we obtain by way of Eq. (2.17) and Eq. (2.18) the expression

$$i\hbar\frac{\partial\hat{\Psi}(r,t)}{\partial t} = \Big[-\frac{\hbar^2\nabla^2}{2m} + U(r,t) + \int \hat{\Psi}^\dagger(r',t)V_{\text{Con}}(r'-r)\hat{\Psi}(r',t)dr'\Big]\hat{\Psi}(r,t). \tag{2.20}$$

Now the Bogoliubov approximation in Eq. (2.5) is employed, transforming the operator $\hat{\Psi}(r,t)$ into the mean field $\Psi(r,t)$. The interbosonic potential matrix element, represented by the integral in Eq. (2.20), is set to g as in Eq. (2.10) and turn Eq. (2.20) into

$$i\hbar\frac{\partial\Psi(r,t)}{\partial t} = \Big[-\frac{\hbar^2\nabla^2}{2m} + U(r,t) + g|\Psi(r,t)|^2\Big]\Psi(r,t) \tag{2.21}$$

which is the GPe. For this model to hold the system needs to be very cold, very dilute and have a large particle number (due to the underlying Bogoliubov approximation). If one wants to utilize Eq. (2.10) to obtain the coupling strength one also needs to introduce the healing length, usually denoted by ξ. The healing length is a measure of length within which the condensate tends to its bulk value. It is given by

$$\xi = \frac{1}{\sqrt{8\pi n a_s}} \tag{2.22}$$

where n is the density of the condensate and a_s is the s-wave scattering length. ξ needs to be larger then the mean distance between particles [1]. This value becomes especially important as we now take the GPe into a quasi 2D realm.

Let us assume that the confining potential U is a harmonic oscillator. If strongly confined in the z-direction the mean-field wave function for the condensate can be written as

$$\Psi_p(r) = \phi(x, y) \times Z(z) \tag{2.23}$$

where the confinement in z-direction is so strong that no movement is allowed. The z-direction wave function is assumed to be that of the lowest level in the one-dimensional harmonic oscillator. In coordinate space that wave function is

$$Z(z) = \frac{1}{\pi^{1/4} l_z^{1/2}} e^{-z^2/2l_z^2} \tag{2.24}$$

where l_z is the oscillator length in z-direction. When the confinement is large enough in the z-direction the distance between particles is $d = 1/\sqrt{n_{2D}}$ where n_{2D} is the density in the xy-plane. Therefore, for the healing length ξ to be much larger then the inter-bosonic distance d one gets

$$\frac{\xi}{d_{particle}} = \sqrt{\frac{l_z}{8\sqrt{\pi} a_s}} \to l_z \gg a_s \tag{2.25}$$

This is a necessary condition for one to be able to use the GPe in its three-dimensional form for 2D systems. This will be taken into consideration during calculations. l_z can also not be too large as that would render the approximation in Eq. (2.23) invalid. Well within these bounds one can use the GPe in Eq. (2.21) with the difference being that the wave function is the effective 2D wave function and the coupling strength is $g = N\sqrt{8\pi}\frac{a_s}{l_z}$ where a_s is the s-wave scattering length, l_z is the oscillator length in z-direction and N is the number of particles. N enters as we normalize the density to one [2]. This definition means that a_s is going to be very small compared to l_z as long as $g < 10^2$ and $N > 10^3$, which we assume them to be in this work.

The GPe can include other inter-bosonic potentials, such as the dipolar, interspecies or spin-orbit coupled potentials. The dipolar interaction will be handled in section 3.2 as it is the main potential studied in this thesis work. The quasi 2D version of the dipole interaction will be the one of greatest interest as it is the potential used in this work. In turn the ability to add further mean-field terms will also help when we look at higher orders of two-particle interactions [1, 2].

Experimental results for the models described above were not obtained until 1995 when an ultra-dilute system of rubidium atoms was cooled with lasers to the point where a condensate were observed [11]. As we shall see in the next section, the first experimental data were quickly followed by other successful experiments performed on ultra-dilute alkali gases [1].

2.3 Experimental realization in extremely dilute alkali gases

The theory of Bose-Einstein condensation was early on used to partly explain the properties of liquid helium [1]. The pure condensate however was not realized until 1995 when three different research groups [11, 13, 14], using magneto-optical cooling techniques, managed to produce ultra-dilute, very cold gases of alkali metals. These gases showed several signs of Bose-Einstein condensation such as a clear density peak at zero-momenta and a high stability (they were observed for times up to 15 seconds) [11, 13, 14].

The magneto-optical trap is a combination of several cooling techniques, including evaporative cooling, laser induced cooling and magnetic trapping [1]. The evaporative cooling technique is the most straightforward and consists of letting high energy particles escape, leaving the entire gas less energetic. The laser techniques involve shooting detuned lasers from six perpendicular or anti-parallel directions, getting higher absorption for particles moving towards the incoming laser light. When the photons are absorbed, the particle is slowed due to momentum conservation [1]. In the magnetic trap the degenerate hyper-fine levels in the atom are manipulated as to have a spatial preference for the middle of the trap. The hyper-fine levels are increased (by the magnetic field) as an atom gets closer to the trap boundary. This creates a force that spatially traps the atoms [1]. There are also other mechanisms at work, such as Sisyphus cooling, where the electrons get pumped into a higher energy level and then spontaneously decay, making the atoms loose energy [1].

In these initial experiments merely contact interactions were studied but in 2005 Ref. [15] created a stable condensate with chromium atoms. The special electric properties of chromium made it possible for researchers to study dipole-dipole interactions in BEC:s. The systems became more tunable as Feschbach resonances became better understood, giving experimentalists the ability to test several strength ratios between the different interactions [4]. In 2011 a condensate was created using the most dipolar atom, dysprosium (Dy) [16] that finally led to experiments in 2015 by Ref. [4] with crystallization of droplets in a dipole interacting BEC. These experiments however led to much more stable droplets and a much more long lived system than anticipated by the GPe [4]. As this finding is the foundation of the area of interest that this thesis handles we now turn our attention to droplet formation and the changes to the GPe that now become necessary to better simulate the observed behaviour.

Chapter 3 | Droplets in dipolar bosonic gases

In 2015 a team at Stuttgart University managed to investigate the area where existing mean field models predicted a collapse of a dipolar BEC [4]. However, the experiments revealed ultra-dilute, self-bound droplet formations. These droplets showed a remarkable stability and ferro-fluid [1] crystalline structure that did not coalesce with theoretical calculations [4]. The stability of the system was attributed to higher order quantum fluctuations, with the Lee-Huang-Yang (LHY) correction term leading to stabilization of the droplets. This in turn started a search for self-bound states where forces such as inter-species or dipolar attractions, as studied in this thesis work, combined with the contact interaction made droplet formation possible [8, 17].

In section 3.1 we will first discuss experimental and theoretical results obtained in the area of quantum droplets. In section 3.2 we will look at the dipole interaction in BEC:s and see how it can be added to the GPe mean field theory. Lastly, in section 3.3 we survey an derivation of the LHY term by Ref. [18] in the framework of Bogoliubov theory.

3.1 Ferro-fluid crystals and self-bound droplet formation

The area of droplet formation in cold atom physics started with the study of strongly dipolar gases in a "pancake" potential, i.e, a harmonic potential more strongly confined in the z-direction. This is not to be confused with a quasi 2D system, as the l_z oscillator length in the pancake system is too large to fulfill the criterion of Eq. (2.23). The ^{164}Dy atoms used in the experiments conducted by Ref. [4] had their contact interaction controlled by strong magnetic fields so that the scattering length resulting from contact interaction became on par with the dipolar interaction (the specifics of the dipole-dipole interaction are discussed in detail in the following section). The standard GPe picture however predicts a destabilization of the condensate at $a_{dd} > a_s$, where a_{dd} is the dipole-dipole scattering length and a_s is the s-wave scattering length. This is due to the dipolar interaction having both regions of repulsive interaction and regions of attractive interaction, leading to a collapse when the attractive part of the dipolar interaction overcomes the repulsive contact interaction. Here, system collapse in the physical sense is the compression of the condensate by the attractive force leading to high densities and temperature increase [4].

The droplets that emerged despite the anticipation of system collapse ordered themselves into a triangular pattern in which the droplets remained stable for about 300 ms. These lifetimes were well beyond what was expected and the enhanced stability of the system was very surprising [4].

To explain these findings two theoretical approaches were taken; quantum fluctuations in the contact interaction, the LHY energy, [8] and three-body interactions [19]. It was however

[1] Ferro-fluids are fluids consisting of highly magnetic atoms or molecules.

concluded that the higher orders of the contact interaction was the main contributor to the stabilization of the droplets with the three-body interaction being the reason for particle losses in the somewhat denser droplets [8]. The LHY correction will be discussed in greater depth in section 3.3 but what can be said is that for the case of the broad "pancake" confined droplets the system has been reproduced numerically for a condensate in three dimensions [8].

Following the above mentioned discoveries the higher order interactions were scrutinized also for two-component gases. In 2015 Petrov suggested that for BEC:s with attractive inter-species interactions larger than the repulsive intra-species interaction, the LHY energy correction could stabilize them. If it did, the system could become a self-bound droplet [5]. This suggestion led to the experimental realization of these droplets in 2016 [6]. The two-component droplets shared a number of features with droplets discovered in the dipolar Dy condensate, with long lifetimes and a lower dependence on the number of particles than expected [20]. Further experimentation is presently being pursued, with an example being the creation of a system were the interspecies and intraspecies contact interaction cancel out and one is left with a system purely dependent on the Lee-Huang-Yang fluctuations [21].

This rapid experimental progress has continued to present date with a recent development being the study of the LHY term in cigar-shaped dipolar Bose-Einstein condensates [22]. Here a self-bound droplet was created in a three-dimensional "cigar" potential. The potentials shape gave way for not only droplet formation but also the formation of oblong stripes much more correlated then the crystalline droplets in the experiment by for example Ref. [4].

To better understand the physical behaviour of these experimental systems we first turn to the dipole interaction. This anisotropic potential let us create systems where the partly attractive dipole force overcomes the contact interaction, making way for systems where the LHY interaction becomes vital to maintain computational stability at the boundaries of system collapse.

3.2 The dipole interaction

The dipole interacting system consists of a number of trapped dipolar particles where the particles are aligned by an external magnetic or electric field. We will only consider magnetic dipoles. For cases of anisotropic trapping potentials the dipoles are often aligned with the z-axis but the dipoles can be tilted, as we will see later in this section.

We start, for convenience, by setting up a system of units where $\hbar = \omega_0 = m = 1$, m being the boson mass, and length is measured in units of the oscillator length l_0 which is $l_0 = \sqrt{\frac{1}{\hbar\omega_0}} = 1$. The dipole-dipole poten-

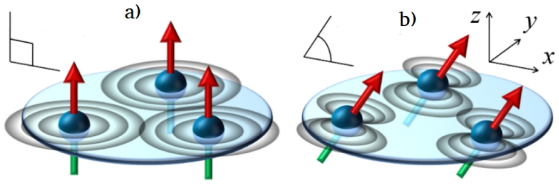

Figure 3.1: The disc shaped quasi 2D dipolar system, as here depicted in the few-body limit. The dipoles are at $\Phi = 90°$ in case a) (dipoles perpendicular to the xy-plane and in case b) the dipole angle $\Phi = 55°$. This figure is taken from Ref. [23].

tial can now be written as

$$V_{dd} = D^2 \frac{1 - 3\cos^2\theta}{r^3} \tag{3.1}$$

where D is the strength of the dipole-dipole interaction, θ is the angle between the dipole and $\mathbf{r}$ which is the distance vector between two dipoles, r being this vectors norm. D is in the magnetic case given by $D = \frac{\mu}{\hbar}\sqrt{\frac{\mu_0 m}{4\pi l_0}}$ which with our choice of units becomes $D = \mu\sqrt{\frac{\mu_0}{4\pi}}$ [23]. For Eq. (3.1) to work it is presumed that all the dipoles are aligned in the same direction.

The matrix elements of Eq. (3.1) governing the form of the effective potential from the dipole interaction is calculated in a similar way as the contact interaction potential in Eq. (2.7). We start with stating that the external potential for the condensate is a harmonic oscillator setting up the dipole potential matrix element as

$${}^{\text{Dip}}V_{j,k,l,m}(\mathbf{r}) = \int dr' dr'' \Psi_j^\dagger(r')\Psi_k^\dagger(r'')V_{dd}(r''-r')\Psi_l(r')\Psi_m(r'') \tag{3.2}$$

where $\Psi_j, \Psi_k, \Psi_l, \Psi_m$ indicate the different single particle harmonic oscillator states. We also note that the integration limit for all integrals are over $\mathbb{R}$. Here one can derive a general three-dimensional expression but as this thesis work focuses on a quasi 2D (as seen in Figure 3.1) approach we will take the route of squeezing the condensate tightly in the z-direction. This tight confinement lets us use the approximation in Eq. (2.23) with the same wave function in z-direction as in Eq. (2.24). This gives us

$${}^{\text{Dip}}V_{j,k,l,m}(\mathbf{r}) = \int d\mathbf{r}_\perp{}' d\mathbf{r}_\perp{}'' \phi^\dagger(\mathbf{r}_\perp{}')\phi^\dagger(\mathbf{r}_\perp{}'')\ {}^{\text{Dip}}V_{\text{eff}}(\mathbf{r}_\perp)\phi(\mathbf{r}_\perp{}')\phi(\mathbf{r}_\perp{}'') \tag{3.3}$$

where $\phi(\mathbf{r}_\perp{}'')$ is the xy-plane wave function in 2.23, $\mathbf{r}_\perp = \mathbf{r}_\perp{}'' - \mathbf{r}_\perp{}'$, and ${}^{\text{Dip}}V_{\text{eff}}(\mathbf{r}_\perp)$ is

$${}^{\text{Dip}}V_{\text{eff}}(\mathbf{r}_\perp) = D^2 \frac{1}{\pi l_z^2} \int dz e^{-z^2/2l_z^2} \frac{1 - 3\cos^2\theta}{r^3} \int d\tilde{z} e^{-2\tilde{z}^2/l_z^2} \tag{3.4}$$

where $z = z'' - z'$, $\tilde{z} = (z'' + z')/2$, $r = r'' - r'$ and l_z is the oscillator length in z-direction. Now, the effective dipolar potential in the xy-plane can be obtained by integrating out the $\tilde{z}$-variable, reducing the effective dipole potential to

$${}^{\text{Dip}}V_{\text{eff}}(\mathbf{r}_\perp) = D^2 \frac{1}{2\sqrt{2\pi} l_z} \int dz e^{-z^2/2l_z^2} \frac{1 - 3\cos^2\theta}{r^3} \tag{3.5}$$

Let's assume that the dipole direction is somewhere in the xz-plane [23]. Then, this system can be rewritten in cylindrical coordinates where we have $(x, y, z) = (r_\perp \cos\phi, r_\perp \sin\phi, z)$. Using the angle between the x-axis and the dipole direction, Φ and the polar coordinate ϕ the value $\cos\theta$ can be calculated by

$$\cos\theta = \frac{1}{r}(r_\perp \cos\Phi\cos\phi + z\sin\Phi). \tag{3.6}$$

Inserting the polar coordinates and Eq. (3.6) into Eq. (3.5) gives us the final expression for the dipole-dipole effective potential:

$$\begin{aligned} {}^{\text{Dip}}V_{\text{eff}}(\mathbf{r}_\perp) = \frac{D^2}{2\sqrt{2\pi} l_z^2} e^{x/2}[(2+2x)K_0(x/2) - 2xK_1(x/2) + \cos\Phi(-(3+2x)K_0(x/2) + \\ (1+2x)K_1(x/2) + 2\cos^2\Phi\cos^2\phi(-xK_0(x/2) + (x-1)K_1(x/2))] \end{aligned} \tag{3.7}$$

where $x = r_\perp/2l_z^2$ and K_0, K_1 are Bessel functions created by integrating over the variable $t = z^2/2a_z^2$. This effective potential can be implemented directly into the the GPe [23].

${}^{\text{Dip}}V_{\text{eff}}$ described above has both repulsive and attractive regions with it being purely repulsive between 90° and $\Phi_{\text{Crit}} = 54.7°$, where Φ_{Crit} is called the critical angle. At this critical point, the dipole-dipole interaction becomes attractive for some regions in the condensate. In the basic model, if the dipole-dipole interaction overcomes the contact interaction, the system collapses. But, as in the case of two-component gases and the droplet crystallization experiments [4, 20], quantum fluctuations might produce stability for the quasi 2D condensate as well. With those words we finally arrive to the heart of the matter: the LHY correction. Presented in 1947 [3], it has been derived in a multitude of ways since [2, 3, 5, 7, 18] for both two-component and dipolar gases. We will start the next section with a general derivation and then discuss the dipole-dipole interaction and its effect on the LHY term, ending our theoretical background and moving on to a brief overview of the method.

3.3 Quantum fluctuations - the higher order interactions in a BEC

In our original derivation of the contact interaction potential in section 2.1 we assumed that all the particles could be found in the lowest state: the condensate. To correct this, we redo the calculations in section 2.1 but we retain the momentum terms [2]. We will start with going through a derivation made in Ref. [18] in 2004. There, the derivation is provided in the framework of a soft potential, i.e, a potential without divergencies close to the atomic boundaries. This can be done as long as the s-wave scattering length of this soft potential is the same as for the "true" interparticle potential [2]. We are still using the same units presented in the previous section.

We begin this by revisiting Eq. (2.8). The interactions of interest are the ones between two states where at least two of the annihilation/creation operators involved are zero momentum based, making them probable enough to affect our outcome. Implementing this we get a modified version of Eq. (2.8)

$$\hat{H} = \sum_q \frac{q^2}{2}\hat{a}_q^\dagger \hat{a}_q + \frac{1}{2V}\,{}^{\text{Con}}V_0 \hat{a}_0^\dagger \hat{a}_0^\dagger \hat{a}_0 \hat{a}_0 + \frac{1}{2V}\sum_{q\neq 0}\Big[\,{}^{\text{Con}}V_{-q}\hat{a}_q^\dagger \hat{a}_{-q}^\dagger \hat{a}_0 \hat{a}_0 + {}^{\text{Con}}V_{-q}\hat{a}_0^\dagger \hat{a}_0^\dagger \hat{a}_q \hat{a}_{-q} + {}^{\text{Con}}V_q \hat{a}_0^\dagger \hat{a}_q^\dagger \hat{a}_q \hat{a}_0 + {}^{\text{Con}}V_0 \hat{a}_0^\dagger \hat{a}_q^\dagger \hat{a}_0 \hat{a}_q + {}^{\text{Con}}V_0 \hat{a}_q^\dagger \hat{a}_0^\dagger \hat{a}_q \hat{a}_0 + {}^{\text{Con}}V_{-q}\hat{a}_q^\dagger \hat{a}_0^\dagger \hat{a}_0 \hat{a}_q\Big]. \tag{3.8}$$

Here we have used Eq. (2.8) and first set $p_1 = 0, p_2 = 0$ obtaining the first term in the sum Eq. (3.8). After this we set $p_1 = q, p_2 = -q$ obtaining the second term in in the sum. The rest of the terms in Eq. (3.8) comes from applying the rule $p_1 + p_2 = q$ where p_1 or p_2 has to be 0. This to have at least two $\hat{a}_0$ operators in each term, as stated above. Adding to this, we use Eq. (2.5) to obtain the approximate number of particles in the condensate, N_0, by using the fact that the total number of particles, N, can be found through Eq. (2.5) by way

of $\int |\Psi|^2 dr = N$. Squaring the number of particles in the condensate state we get

$$N_0^2 = N^2 - 2N \sum_{q\neq 0} \hat{a}_q^\dagger \hat{a}_q + \big(\sum_{q\neq 0} \hat{a}_q^\dagger \hat{a}_q \big)^2. \tag{3.9}$$

The last square in Eq. (3.9) can be discarded as it is very small, leaving us with the following expression for N_0,

$$N_0^2 \approx N^2 - 2N \sum_{q\neq 0} \hat{a}_q^\dagger \hat{a}_q \tag{3.10}$$

where N is the total number of particles. Inserting Eq. (3.10) into Eq. (3.8) a number of terms cancel and all small terms of the form $\sum_{q\neq 0} \hat{a}_p^\dagger \hat{a}_p \hat{a}_q^\dagger \hat{a}_q$ are discarded. This leaves us with the Hamiltonian

$$\hat{H} = \frac{Nn}{2} \, {}^{\mathrm{Con}}V_0 + \sum_q \frac{q^2}{2} \hat{a}_q^\dagger \hat{a}_q + \frac{n}{2} \sum_{q\neq 0} \, {}^{\mathrm{Con}}V_q (\hat{a}_q^\dagger \hat{a}_{-q}^\dagger + \hat{a}_{-q}\hat{a}_q + 2\hat{a}_q^\dagger \hat{a}_q) \tag{3.11}$$

Important to note here is that ${}^{\mathrm{Con}}V_q = {}^{\mathrm{Con}}V_{-q}$ [18].

To study this Hamiltonian, we turn to the Bogoliubov transformation. First, one creates a Hamiltonian for each state dependent on q on the form

$$H_q = A_q + B_q(\hat{a}_q^\dagger \hat{a}_{-q}^\dagger + \hat{a}_q \hat{a}_{-q} + \hat{a}_{-q}^\dagger \hat{a}_q^\dagger + \hat{a}_{-q}\hat{a}_q) + C_q(\hat{a}_q^\dagger \hat{a}_q + \hat{a}_{-q}^\dagger \hat{a}_{-q}) \tag{3.12}$$

where $A_q = \frac{n^2}{2} \frac{{}^{\mathrm{Con}}V_q^2}{q^2/2}$, $B_q = \frac{n}{2} \, {}^{\mathrm{Con}}V_q$ and $C_q = n \, {}^{\mathrm{Con}}V_q + \frac{q^2}{2}$. Here we have made use of what Weiss *et al.* [18] refers to as a "fat 0" when using ${}^{\mathrm{Con}}V_0$. Instead of setting ${}^{\mathrm{Con}}V_0 = 4\pi a_s$ we use

$${}^{\mathrm{Con}}V_0 = 4\pi(a_s + a_2) + \frac{1}{V} \sum_{q\neq 0} \frac{{}^{\mathrm{Con}}V_q^2}{q^2} \tag{3.13}$$

where a_2 is the second order term in the Born series discussed in chapter 2. The sum in Eq. (3.13) and the second order Born series term cancel each other, forming a "fat 0" and allow us to set $A_q = \frac{n^2}{2} \frac{{}^{\mathrm{Con}}V_q^2}{q^2/2}$, which will prevent unphysical results encountered by Weiss *et al.* in Ref. [18].

We now want to diagonalize Eq. (3.12) as follows

$$H_q = \alpha(q) + \epsilon(q) \beta_q^\dagger \beta_q \tag{3.14}$$

where β_q is a creation/annihilation operator for a quasi-particle with energy $\epsilon(q)$ and $\alpha(q)$ is the energy shift. $\alpha(q)$ can be seen as the ground state energy for the quasi-particles in a harmonic oscillator [18]. The operator β_q has to follow the commutation rules of Bose statistics and can be written as a combination between a_{-q} and a_q in the following fashion:

$$\beta_q = u_q \hat{a}_q + w_q \hat{a}_{-q}^\dagger \tag{3.15}$$

$$\beta_q^\dagger = u_q \hat{a}_q^\dagger + w_q \hat{a}_{-q} \tag{3.16}$$

By using Eq. (3.15) and (3.16) and rewriting Eq. (3.12) in the form of Eq. (3.14) we find that the quasi-particle energy ϵ, is

$$\epsilon(q) = \sqrt{\left(\frac{q^2}{2}\right)^2 + n\ {}^{\text{Con}}V_q q^2} \tag{3.17}$$

with the energy shift α becoming

$$\alpha(q) = \frac{1}{2}\Big[\epsilon(q) - \frac{q^2}{2} - n\ {}^{\text{Con}}V_q\Big] + \frac{n^2}{2}\frac{{}^{\text{Con}}V_q^2}{q^2/2} \tag{3.18}$$

The Hamiltonian in Eq. (3.11) can now be written as

$$\hat{H} = \frac{Nn}{2}\ {}^{\text{Con}}V_0 + \sum_q H_q. \tag{3.19}$$

At this point we want to look at all the Hamiltonian terms that are independent of the momentum q. Therefore we discard any terms in the Hamiltonian, Eq. (3.19), that are dependent on the momentum of a state, i.e β_q dependent terms. This removes the quasi particle energies, ϵ, which is physically motivated as higher momentum states will not be occupied in any larger extent. The energy shift, brought about by higher momentum states, remains the same no matter what state we apply the operator to. This leaves us with the energy per particle

$$\frac{E}{N} = \frac{1}{2}\ {}^{\text{Con}}V_0 n + \frac{1}{nV}\sum_{q\neq 0}\alpha(q) \tag{3.20}$$

where n is the density and V is the volume of the system. At this point we reaffirm that this is being done at an ultra-dilute density, letting us Taylor expand the sum of energy shifts, $\alpha(q)$, around $n = 0$ as follows

$$\sum_{q\neq 0}\alpha(q) = \sum_{q\neq 0}\alpha(q)\Big|_{n=0} + \sum_{q\neq 0}\frac{\partial}{\partial n}\alpha(q)\Big|_{n=0} n + \frac{1}{2!}\sum_{q\neq 0}\frac{\partial^2}{\partial n^2}\alpha(q)\Big|_{n=0} n^2 + \dots \tag{3.21}$$

The zeroth, first and second order terms of this Taylor expansion become 0. The third term becomes an infrared-divergent integral which Weiss *et al.* describe as a "naive attempt to consider" [18]. Instead we use the fact that ${}^{\text{Con}}V_q$ is bounded and that we therefore can use the following expression:

$$\sum_{q\neq 0}\frac{\partial}{\partial\sqrt{n}}\frac{\partial^2}{\partial n^2}\alpha(q)^2 \tag{3.22}$$

Using Eq. (3.18) for $\alpha(q)$ we find Eq. (3.22) to be

$$\sum_{q\neq 0}\frac{\partial}{\partial\sqrt{n}}\frac{\partial^2}{\partial n^2}\alpha(q)^2 = \lim_{n\to 0}\sum_{q\neq 0}\frac{3\big(\frac{q^2}{2}\ {}^{\text{Con}}V_q\big)^3\sqrt{n}}{\Big[(\frac{q^2}{2})^2 + 2n\ {}^{\text{Con}}V_q\frac{q^2}{2}\Big]^{5/2}} \tag{3.23}$$

The boundness of ${}^{\mathrm{Con}}V_q$ means that the sum in Eq. (3.23) will converge and we can rewrite it as an integral over q:

$$\sum_{q\neq 0}\frac{\partial}{\partial\sqrt{n}}\frac{\partial^2}{\partial n^2}\alpha(q)^2=\lim_{n\to 0}\frac{V}{2\pi}\int d^3q\frac{3\left(\frac{q^2}{2}\ {}^{\mathrm{Con}}V_q\right)^3\sqrt{n}}{\left[(\frac{q^2}{2})^2+2n\ {}^{\mathrm{Con}}V_q\frac{q^2}{2}\right]^{5/2}} \tag{3.24}$$

where V is the volume of the system that arises from the density in phase space. This integral becomes simplified substituting the momentum vector $q=\sqrt{2m\ {}^{\mathrm{Con}}V_0y^2n}$ where y is a dimensionless variable. We also use that in the thermo dynamic limit, $\lim_{n\to 0}\frac{{}^{\mathrm{Con}}V_q}{{}^{\mathrm{Con}}V_0}=1$ and thus the problem reduces to

$$\sum_{q\neq 0}\frac{\partial}{\partial\sqrt{n}}\frac{\partial^2}{\partial n^2}\alpha(q)^2=\lim_{n\to 0}\frac{3V}{2\pi^2}(2)^{3/2}\ {}^{\mathrm{Con}}V_0^{5/2}\int_0^\infty dy\frac{y^3}{(y^2+2)^{5/2}} \tag{3.25}$$

where the integral is simply equal to $\sqrt{2}/3$. Now we use this as any Taylor expansion term and see that its expansion polynomial (with factorials) is $\frac{4}{15}n^{5/2}$ as

$$\frac{\partial}{\partial\sqrt{n}}\frac{\partial^2}{\partial n^2}\frac{4}{15}n^{5/2}=1 \tag{3.26}$$

Now, we combine the polynomial with the coefficient in Eq. (3.25) and change ${}^{\mathrm{Con}}V_0$ to the result in Eq. (2.10). We also remember the factor in-front of the shift energy sum in Eq. (3.20). Combining all this leads to the expression

$$\frac{1}{nV}\sum_{q\neq 0}\frac{\partial}{\partial\sqrt{n}}\frac{\partial^2\alpha(q)}{\partial n^2}\Big|_{n=0}\times\frac{4}{15}n^{5/2}=2\pi a_s\frac{128}{15\sqrt{\pi}}n\sqrt{na_s^3}. \tag{3.27}$$

This energy shift can now be added to the the contact interaction energy and is called the LHY energy correction [18].

The derivation above is from 2004 Ref. [18] but the same result has been obtained before, most notably as its first iteration in 1947 by Lee, Huang and Yang [3]. In the 2004 paper a soft potential was used, as was also done in Pitaevskii and Stringaris Ref. [2]. Lee, Huang and Yang however used a hard sphere potential, but obtained the same results [2, 3, 18].

LHY energy corrections have also been derived for systems with other density dependent interaction energies. In the case of the two-component gas Petrov derived a term dependent on the interspecies coupling [5] and in the case of the dipolar condensate Lima and Pelster produced LHY correction term in 2012 [7].

The dipolar LHY correction has the same form as Eq. (3.27) with a notable difference being the equation $Q_5(\epsilon)$ giving us the following expression for the dipolar LHY energy correction per particle

$$\frac{E_{LHY}}{N}=2\pi a_s\frac{128}{15\sqrt{\pi}}n\sqrt{na_s^3}Q_5(\varepsilon) \tag{3.28}$$

where $Q_5(x)=(1-x)^{5/2}\ {}_1F_2(-\frac{5}{2},\frac{1}{2};3/2;\frac{3x}{x-1})$ and ${}_1F_2$ is the hyper geometric function. Lima and Pelster call this term the "dipolar enhancement of the correction" [7] and it is the direct

result of the dipole potential Eq. (3.1). There ϵ is the relative strength between the coupling interaction and the dipole-dipole interaction strength seen in Eq. (3.1), where ϵ is given by

$$\epsilon = \frac{4\pi D^2}{3g} \tag{3.29}$$

and notably ϵ is confined between 1 and 0 as the hypergeometric function is only defined in said interval.

The implication of lower dimensionality on the LHY term (in the two-component case) has been discussed by Petrov and Astrakharchik [17] and Zin *et al.* [26]. Here we see that there are differences to the LHY term, most notably the adding of an logarithm term, but it mostly affects the LHY strength for densities below $n < 0.3$, the norm of n being 1. Though this might have consequences for the calculations, especially in regions towards the droplet surface, the three-dimensional LHY term will still be used in this thesis work. The aim of this project is merely to test the stabilization by the three-dimensional correction in order to potentially compare with the 2D case later on.

We now turn to the numerical method used. The code will not be discussed in-depth, but focus will instead be on the method and how the LHY term is implemented.

Chapter 4 | Solving the Gross-Pitaevskii equation for dipolar Bose-Einstein condensate droplets in two-dimensions

The theoretical study of the GPe is to a large extent dependent on numerical methods. There are several approaches to solving it, with the fourth order, split operator imaginary time method being one of the more efficient ones when it comes to obtaining the ground state energy and density [9, 24]. Implementing the LHY correction in this framework is simple as it only adds to the general mean field potential. In section 4.1 we go through the method, quickly reviewing its basic structure. In section 4.2 the LHY implementation is handled with some discussion around the choice of parameters and how to counteract at least some of the discrepancies coming from using the three-dimensional LHY term in a quasi-2D setting.

4.1 The fourth order, split operator imaginary time method

To solve the GPe, a fourth order, split operator, imaginary time method is used [9]. It involves iterating in imaginary time, minimizing the energy of the system and obtaining the wave function. In our case the external potential is a harmonic oscillator trap, with a quasi-2D shape.

Let's say that we have a rotating single particle in a harmonic oscillator trap, squeezed in the z-direction. The Hamiltonian will be described as (using atomic units $\hbar = m = \omega_0 = 1$)

$$\hat{H} = \frac{1}{2}(\hat{p}_x^2 + \hat{p}_y^2) + \frac{1}{2}\omega(\hat{x}^2 + \hat{y}^2) - \Omega(\hat{x}\hat{p_y} - \hat{y}\hat{p_x}) \tag{4.1}$$

where $\hat{p}_i$ is the momentum operators, $\hat{x}$ and $\hat{y}$ the spatial operators, ω is the harmonic oscillator strength and Ω is the rotational momentum strength. In the method used this Hamiltonian can be exchanged for a GPe version with the only adage to 4.1 being a contact interaction term. The momentum, rotational and spatially dependent parts has the same form in the single particle case and the mean-field description.

So let's look at the mean-field time propagation. The time translation operator for this system is simply $e^{it\hat{H}}$, where t is the time and $\hat{H}$ is the same form as the Hamiltonian in Eq. (4.1), with an added contact interaction. As we want to use imaginary time-steps to find the lowest energy state [9], we rewrite the time translation operator as $e^{-\tau\hat{H}}$. The Hamiltonian is however not diagonalized, leading us to approximate it as a power series, splitting the operator. We do this to the fourth order giving us

$$e^{-\tau H} = e^{-\frac{1}{6}\tau V_{Eff}} e^{-\frac{1}{2}\tau T} e^{-\frac{2}{3}\tau \tilde{U}} e^{-\frac{1}{2}\tau T} e^{-\frac{1}{6}\tau V_{Eff}} + \mathcal{O}(5), \tag{4.2}$$

where V_{Eff} is the effective potential

$$V_{\text{Eff}} = \frac{1}{2}\omega(x^2 + y^2) - \frac{1}{2}\Omega(x^2 + y^2) + g|\phi|^2, \tag{4.3}$$

where g is the contact interaction strength and ϕ is the condensate wave function, T is the kinetic energy

$$T = \frac{1}{2}(p_x + \Omega y)^2 + \frac{1}{2}(p_y - \Omega y)^2 = \frac{1}{2}(T_x + T_y) \tag{4.4}$$

and $\tilde{U}$ is

$$\tilde{U} = V + \frac{1}{48}\tau^2 V_{\text{Eff}}[V_{\text{Eff}}, T]. \tag{4.5}$$

For the 2D case $\tilde{U}$ can be rewritten

$$\tilde{U} = V + \frac{1}{48}\tau^2\Big[\big(\frac{\partial U}{\partial x}\big)^2 + \big(\frac{\partial U}{\partial y}\big)^2\Big]. \tag{4.6}$$

The kinetic energy T is still not diagonalized however. But as it is on the same form as a harmonic oscillator Hamiltonian (two quadratic operators added) we can use the exact solution to the harmonic oscillator [24], giving us

$$e^{-\tau T} = e^{-\tau\frac{1}{2}(T_x+T_y)} = e^{\frac{1}{2}C_v T_x} e^{\frac{1}{2}C_t T_y} e^{\frac{1}{2}C_v T_x} \tag{4.7}$$

To calculate the kinetic energy we employ a system of Fast Fourier transforms, applying $e^{-\frac{1}{2}\tau T}$ to the wave function by first Fourier transforming the wave function $\phi(x, y)$ into $\tilde{\phi}(p_x, y)$ and multiplying by the partial evolution operator $e^{-\frac{1}{4}C_v(p_x+\Omega y)^2}$. After that we transform the wave function back into x-space and then into p_y-space and multiplying with $e^{-\frac{1}{4}C_T(p_y-\Omega x)^2}$. Transforming our way back to $\tilde{\phi}(p_x, y)$ we once again multiply by $e^{-\frac{1}{4}C_v(x+\Omega y)^2}$ and have now evolved the function with regards to the kinetic energy [24]. This shows why we create the operators T_x and T_y, as this reduces the amounts of Fast Fourier transforms that are needed during one iteration.

C_V and C_T are variables that are found to be

$$C_V = \frac{\cosh(\Omega\tau) - 1}{\Omega\tau\sinh(\Omega\tau)} \tag{4.8}$$

$$C_T = \frac{\sinh(\Omega\tau)}{\Omega\tau} \tag{4.9}$$

with Ω being the rotation of the system. This could be problematic if Ω is set to zero, as it will in this case. However, for small τ the variables C_V and C_T can be Taylor expanded, giving us $C_v = 1/2$ and $C_t = 1$ at $\Omega \to 0$ [9]. After these iterations the wave function has to be normalized as the time translation operator is not norm conserving.

As we also have a dipole-dipole interaction in this particular case and the effective potential functional V_{Eff} is therefore

$$V_{\text{Eff}} = V_{\text{Ext}} + V_{\text{Con}} + V_{\text{Dip}} - \frac{1}{2}\Omega(\hat{x}^2 + \hat{y}^2) \tag{4.10}$$

where V_{Ext} is the external potential (in our case a harmonic oscillator), V_{Con} is the contact interaction potential defined in Eq. (2.21) and V_{Dip} is the dipolar interaction defined in Eq. (3.7). The part furthest to the right is there to account for how T_x and T_y were defined and prevent double counting. Last but not least, the LHY term has to be added to the effective potential above. This however will be done with the three-dimensional functional in 2D which leads to some changes to Eq. (3.28).

4.2 Implementing the Lee-Huang-Yang term

The local LHY correction for a BEC that will be implemented is

$$\frac{E_{LHY}}{N} \cdot n \cdot dr = \frac{2\pi a_s}{m} \frac{128}{15\sqrt{\pi}} n^2 \sqrt{n a_s^3} Q_5(\varepsilon) dr \tag{4.11}$$

where E_{LHY}/N is the LHY energy correction per particle arrived at in section 3.3. We note the function $Q_5(\varepsilon)$, the spatial infinitesimal dr and that n has norm N [7]. As our calculations are based on the 2D coupling strength $g = \frac{N\sqrt{8\pi}a_s}{l_z}$ Eq. (4.11) becomes in terms of g

$$E_{LHY} \cdot n_1 \cdot dr = g l_z \frac{35}{15} \sqrt{\frac{l_z^3 g^3}{\sqrt{2}\pi^{\frac{3}{2}}}} n_1^{\frac{5}{2}} dr \tag{4.12}$$

where n_1 is the 3D density with norm 1 and we set $\hbar = m = 1$. The coupling constant for the LHY correction term in the GPe is then obtained by taking the first derivative of the right hand side of Eq. 3.28 with regards to n_1 and removing the infinitesimal dr. However, the density in Eq. (4.12) is based of the 3D wave function, $\psi(r)$ and the code has the 2D wave function, $\phi(x, y)$, implemented. This is not a problem when looking at the basic coupling strength in Eq. (2.21) as the function in z-direction, $Z(z)$, is normalized, i.e $\int dz |Z(z)|^2 = 1$, giving that

$$\int dr |\Psi(r)|^2 = \int \int dx dy |\phi(x, y)| = 1 \tag{4.13}$$

In the basic GPe, when calculating the contact interaction energy, the wave function is to the power of four as

$$\frac{1}{2} g \int dr |\Psi(r)|^4 \tag{4.14}$$

for which the integral $\int dz |Z(z)|^4 = \frac{1}{\sqrt{2\pi} l_z}$. This is solved already through the rewriting of the three-dimensional g factor for 2D. We recall Eq. (2.23) and Eq. (2.24) and look at the contact interaction energy in terms of g_{3D} in a quasi 2D setting, integrate out z and get

$$\frac{1}{2} g \int dr_\perp \int dz |\phi(x, y)|^4 \times |Z(z)|^4 = \frac{1}{2} g \frac{1}{\sqrt{2\pi_z}} \int dr_\perp |\phi(x, y)|^4 \tag{4.15}$$

Using Eq. (2.10) for the three-dimensional g we get

$$\frac{1}{2} g \int dr_\perp \int dz |\phi(x, y)|^4 \times |Z(z)|^4 = \frac{1}{2} \frac{\sqrt{8\pi} a_s}{l_z} \int dr_\perp |\phi(x, y)|^4 \tag{4.16}$$

where $\frac{\sqrt{8\pi}a_s}{l_z}$ is the 2D coupling constant, also referred to as g. So, as we have corrected for the integrated $Z(z)$ for the contact interaction and its energy, we do the same for the LHY terms. We therefore calculate a term for both $\int dz|Z(z)|^3$, that will be multiplied with the LHY functional in our extended GPe and $\int dz|Z(z)|^5$ that will be used to calculate the LHY energy E_{LHY}. These correction terms are $\int dz|Z(z)|^3 = \sqrt{\frac{2}{3a_z}\frac{1}{\pi^{1/4}}}$ and $\int dz|Z(z)|^5 = \sqrt{\frac{2}{5a_z^{3/2}}\frac{1}{\pi^{3/4}}}$ [25].

The intervals chosen for D, the dipolar interaction strength, for our calculations are between 0.25 and 2 [a.u]. These will in turn be checked for collapses for the lowest possible g, given by Eq. (3.29). If collapses are found an LHY term will be implemented to see if it can provide a remedy. These calculations will then be done within a grid of points, a mesh, where each point represents a local density. The number of mesh-points and the spatial step-length used will be discussed as we now turn to the results.

Chapter 5 | Results

The results in this Bachelor thesis work are not yet conclusive but gives a brief overview of the systems at the parameter region of collapse, both for dipolar and contact interaction. The units used to measure the basic properties of these systems are defined by setting $\hbar = \omega_0 = m = 1$. ω_0 is the unit of energy and m is the mass of the particles. Length is here measured in units of $l_0 = \sqrt{\frac{1}{\hbar\omega_0}} = 1$. These units will be referred to as [a.u], for atomic units, and with pre-factors explaining the type of unit. The number of mesh points are for all calculations 512×512 and the oscillator length in z-direction, l_z, is always set to 0.1.

First, we will look at systems with low values of D probing the stability of the GPe, without a LHY correction term. With this information systems are chosen and checked for the angle Φ at which the GPe breaks down. Lastly we will look at the effect of the LHY in the cases where the GPe collapses and becomes unphysical. At times several spatial step lengths are used in tandem but if nothing else is said the standard length is $dl = 0.1$.

Convergence in these tests will be determined by the system total energy. At 5000 iterations convergence to the 12 decimal was almost always achieved, with some exceptions. Non-convergence in energy indicates a system without stable groundstate and will be counted as unphysical and a possible sign of collapse. A collapse can however have a false, yet numerically converged energy, which is why densities will be be checked for unphysical behaviour. If either non-convergence or unphysical densities are present in a result it will be deemed as erroneous.

5.1 Collapsing systems

Starting at lower values of the dipole-dipole interaction strength D we find that collapse of the condensate is avoided even at the point where the dipoles lie in the xy-plane, as seen in Table 1. In the first run $D = 0.25$, the harmonic confinement is $\omega = 0.5$ (in units of ω_0) and the contact interaction, g, has a smallest possible value of around ~ 0.27, as defined by Eq. (3.29). The kinetic energy is approximately one order of magnitude larger than the interaction terms. The same is true for $D = 0.5$, though the interaction energies are now at least on the same scale as the kinetic energy, as can be seen in Table 5.1. It is not until $D = 1.0$ that a collapse can be observed. Even though the energy converges numerically for $D = 1.0$, the high energies and the density being confined to a decreasing number of mesh points leading to an unphysical limit, indicates a collapse.

Table 5.1 shows the trapping energy, E_{Trap}, becoming smaller than the dipolar energy E_{Dip}, thus shaping the 2D density. The dipole interactions anisotropy leads to interesting 2D-density functions where the xz-density profile is narrower than the yz-density profile, which is illustrated in Figure 5.1 and Figure 5.2. These asymmetries are however not seen in the case of low D:s or for systems where the dipoles are not tilted sufficiently. Most systems therefore have the same characteristics as Figure 5.1 and 5.2 but are less pronounced, as Figure 5.2 shows a system very near a collapse.

The dipole-dipole interaction is strongly attractive for the data shown in Figure 5.2. This is however not sufficient to create self-bound condensates, i.e to confine the gas without the presence of a trap. All release tests of collapsing systems without a LHY correction term led to "leakage", see Figure 5.6 for an example, outside the mesh and thus unphysical results.

D [a.u]	g [a.u]	E_{Kin} [a.u]	E_{Trap} [a.u]	E_{Dip} [a.u]	E_{Int}[a.u]
0.25	0.27	0.2373	0.2340	-0.04812	0.01159
0.5	1.05	0.3560	0.1785	-0.2583	0.06150
0.75	2.36	1.234	0.05951	-1.838	0.4703
1.0	6.55	242.9	0.001399	-350.8	90.98

Table 5.1: Changing the dipole-dipole interaction strength D, $\Phi = 0°$, the contact interaction g is at minimum level for each D. The oscillator confinement frequency was $\omega = 0.5$ for all calculations.

Before testing the GPe with LHY term added a set of parameters were more thoroughly tested to find angles where the GPe breaks down. The variables were chosen as to make room for changing the contact interaction g and dipole tilt angle Φ during further tests and as a start $D = 1.0$ was chosen and g set to 20.

At $D = 1.0$, $\omega = 4$ and coupling strength $g = 20$ the system did not collapse for any values of the angle Φ. This system had the dipole angle Φ tilted in the xz-plane to change the dipole interaction energy in search of a collapse. Φ, ranging between 90° and 0°, was lowered with 5° increments obtaining a converged state for each angle. The dipole-dipole interaction deformed the system as was expected but never reached the anisotropy displayed in Figuren 5.2 or 5.3. Instead the system was stable for all possible angles Φ. This indicates that interval of collapse is bounded at both a lower limit for g set by Eq. (3.29) and an upper limit where the dipole-dipole energy cannot overcome the contact interaction energy.

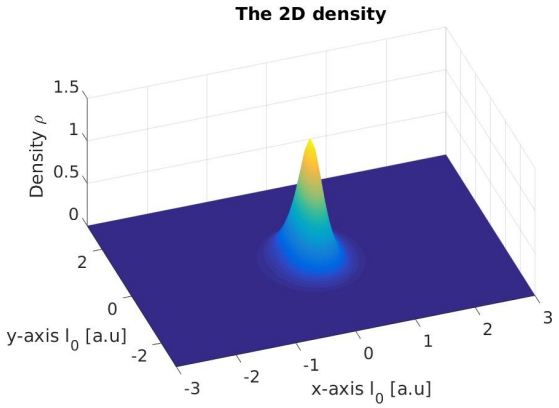

Figure 5.1: The 2D density in a mesh. The anisotropic nature of the dipole interaction makes the condensate oblong, making it longer in the y direction. As we later look at density profiles those are slices of the total density, either seen from the x or the y-axis.

To still obtain a large interval of g values to work with, D was increased to 2 and the same procedure was conducted to find a collapse, which was observed at 33.6°. The deformation of the density for $D = 2, g = 20, \omega = 4$ at $\Phi = 33.7°$ can be seen in Figure 5.2.

For $D = 2, g = 20, \omega = 4$, two different step lengths, $dl = 0.05$ and $dl = 0.1$, were used. The results discussed above and displayed in Figure 5.2 are for step length 0.05. With

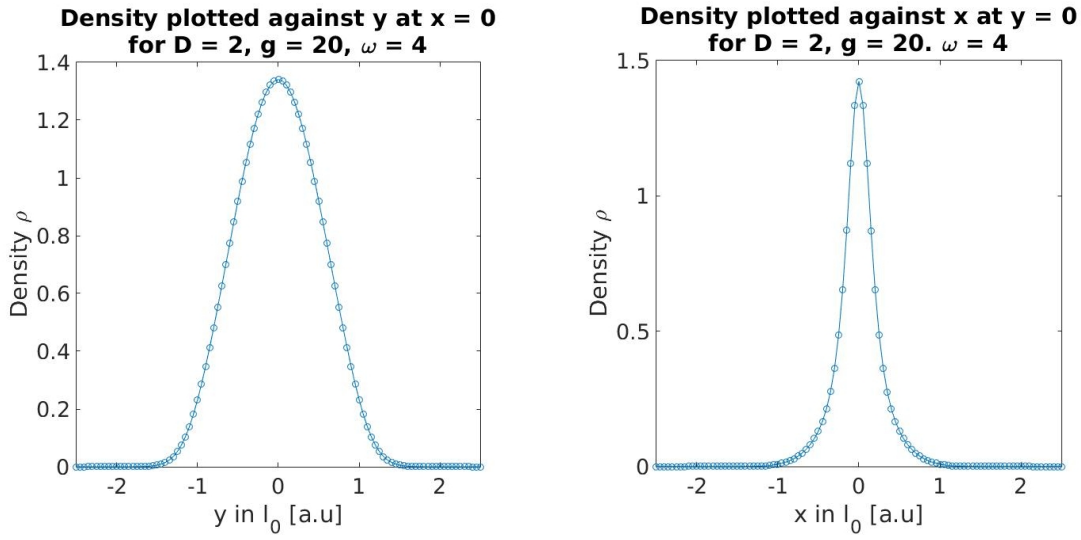

Figure 5.2: The density profiles for the yz-plane (left) and xz-plane (right) for $D = 2, g = 20, \omega = 4$. The anisotropic nature of the dipole-dipole interaction can be seen in the squeezing of the density in x-direction, as compared to the yz density profile that has a Gaussian shape.

$dl = 0.1$ the system collapses at 33.4°, with a possible reason for the increased stability being artifacts originating from the condensate being spread over to few mesh points. This might seem as a strong case for always using a higher resolved picture. This however also has its problems as potential droplets will be released from the trap and are usually bigger than the trapped condensate. The difference between a droplet that is too big for the mesh and a condensate that has dissipated is very small making the results indistinguishable and therefore both step lengths are used simultaneously. Note also that the densities are similar for both step lengths. The same method was then employed for $D = 2, g = 40, \omega = 4$, with similar results. Before the condensate collapsed at $\Phi = 24.0°$ the system showed density profiles resembling those in Figure 5.2.

Testing to see if these collapsing systems could do without both trap and LHY term and still be self-bound showed that they could not. Either the densities of these systems "leaked" out to the borders of the mesh or collapsed into a small number of mesh points, both being unphysical results. We therefore added the LHY term to our simulations and determined if a collapse could be stopped by it.

5.2 Implementation of the LHY correction

For the LHY implementation the wave function of GPe stable systems were used as an initial guess for the iterations of the GPe. Runs were made for the angle 0.1° before collapse. In the case of the condensate displayed in Figure 5.3 this meant an initial run at 37.7° and then decreasing the angle by increments of 0.1° until collapse or $\Phi = 0$. For the system $D = 2.0$ and $g = 20$, with step length 0.05 and 0.1, collapse was indeed stopped as can be seen in Figure 5.3 where the xz-plane density profile from the non-LHY calculations, at $\Phi = 33.7°$, is compared with the xz density profile of the LHY implemented GPe at $\Phi = 33.7°$ (step

length set to 0.05 for both runs). Here we see the LHY term broadening the thin peak in the the xz-plane, lowering the maximum value of the density from 1.4 to approximately 0.9. The sharp peaks occured for both step lengths used.

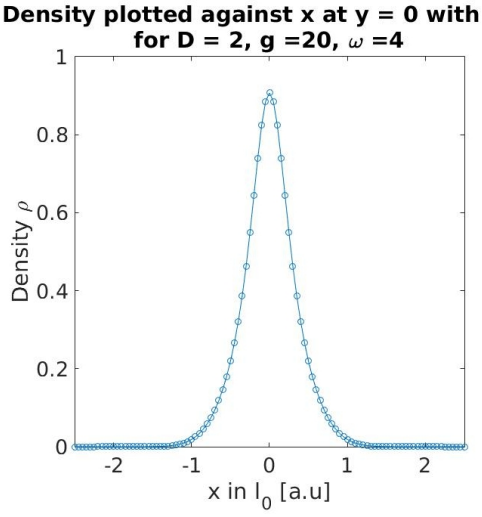

(a)

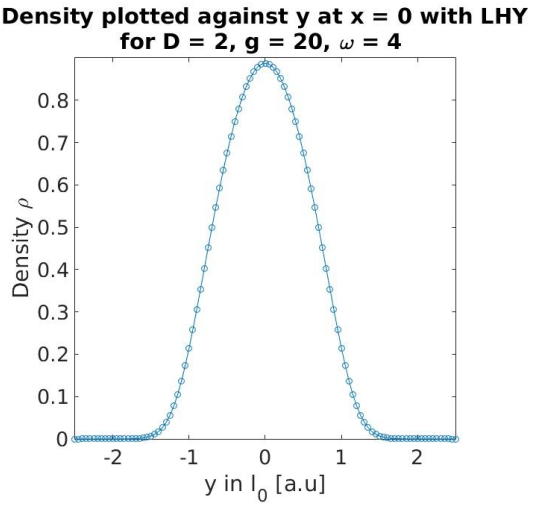

(b)

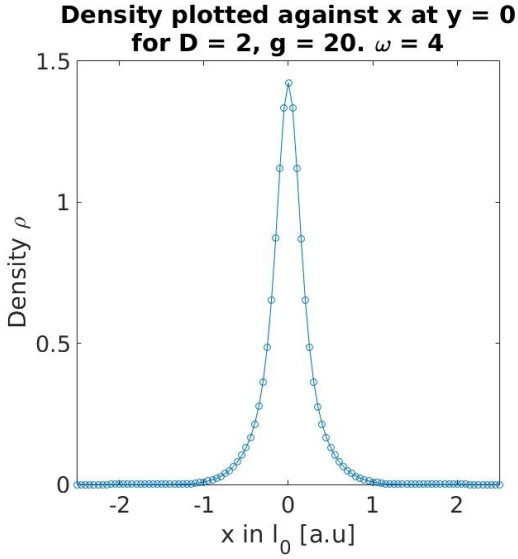

(c)

Figure 5.3: The comparison between the xz-plane density profile for LHY implemented, (a), and the basic GPe, (c). The graphs are for $D = 2, g = 20, \omega = 4$ with the LHY density having the angle $\Phi = 33.7°$ and basic GPe density being at $\Phi = 33.7°$. The difference between (a) and (c) is due to the LHY potential. b) shows the yz density profile for the LHY condensate, with a familiar Gaussian shape.

The LHY condensate at $g = 20, D = 2$ collapses at 33.1°, increasing the range of stability with 0.5°. The LHY energies are consistently at values approximately one order of magnitude smaller than other leading energy terms. It is however pronounced enough to cause a change

in shape of the condensate, as seen in Figure 5.3.

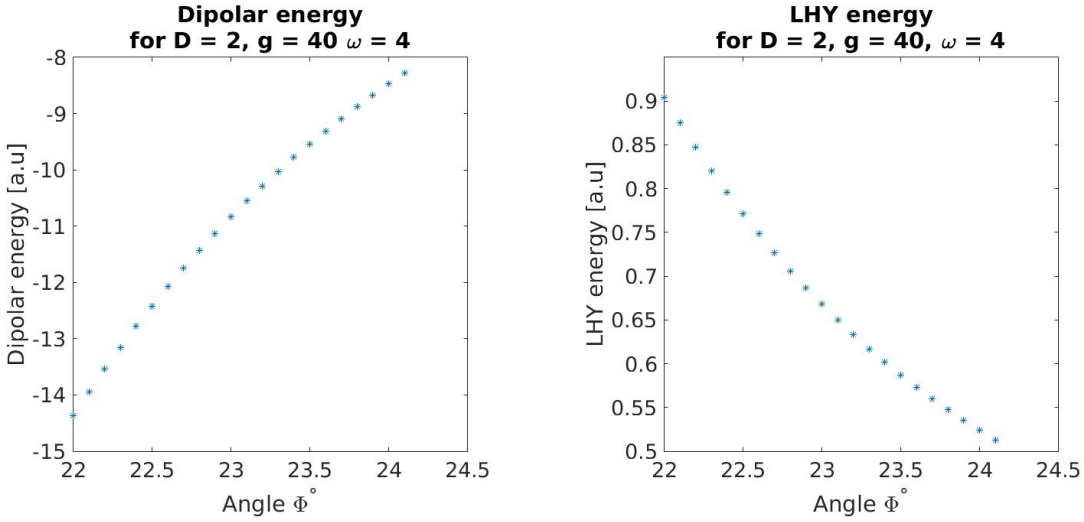

Figure 5.4: The dipole and LHY energy for the GPe with LHY correction. All angles are lower than the angle of collapse for GPe without LHY. The quickening pace of energy decrease for the dipolar energy is followed by the breakdown of the GPe and unphysical solutions.

To continue these tests, the parameters were set to $D = 4, g = 40$ and $\omega = 4$. This system proved even more stable with the interval of stability being increased by 2.1°, going from collapse at $\Phi = 24.0°$ to collapse at $\Phi = 21.9°$.

The collapse at $\Phi = 21.9°$ differs from the previously studied cases. The steep slope of the dipolar energy and LHY energy, see Figure 5.4, is followed by the break down of the GPe with LHY term implemented. This breakdown however is a non-convergence in energy, with the density still being seemingly stable for the parameters discussed above. The energy started to fluctuate and lowering the dipole tilt even further led to the yz density profile starting to collapse at $\Phi = 21.7°$ as shown in Figure 5.5.

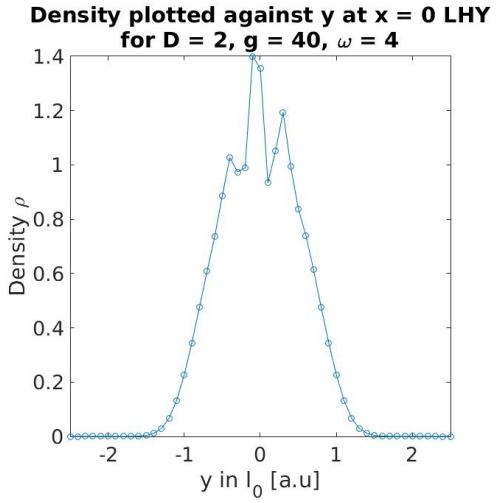

Figure 5.5: The density becomes unstable for $D = 2, g = 40, \omega = 4, \Phi = 21.7°$. This density profile has lost its Gaussian shape displayed in Figure 5.2 and 5.3 b) and the function behaves somewhat discontinuous. The energy for this system has already stopped converging and started fluctuating at $\Phi = 29.9°$

.

At this stage, the wave functions for some of the lower lying angles Φ were then used as initial guess for runs where the trap was turned of. This lead to leakage as shown in Figure 5.6 that represents one of those simulations. This may indicate that the external trap is partly involved in collapsing

the system and that even lower angles are needed to actually self-bind a droplet. This is also suggested by the density profiles of the droplet runs as their peak density value increased for lower angles. But as they are non-physical solutions they must be disregarded. The runs made with $\omega = 0$ were made for $D = 2, g = 40$ at Φ set to 22.5°, 22.3° and 22.1°.

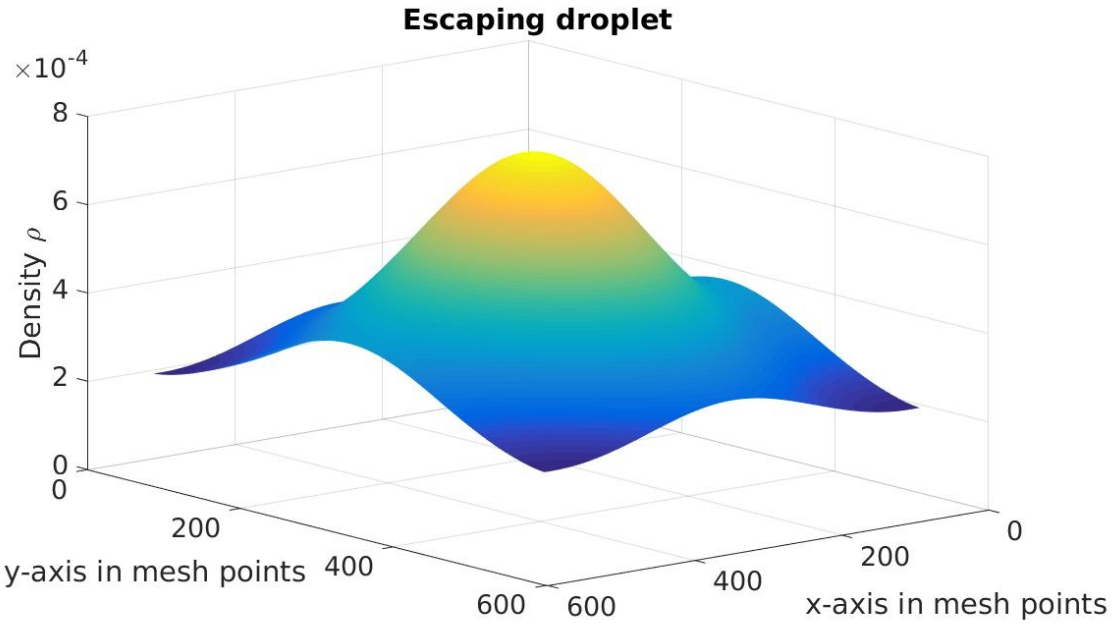

Figure 5.6: Density escaping the mesh. When removing the harmonic trap ω the mesh size is shown to be too small, rendering the results unphysical. This Figure shows the density resulting from $D = 2$, $g = 40$ and $\Phi = 22.1°$

.

5.3 Summary

To summarize, we have confirmed that for high enough values of D the GPe breaks down. This can be stopped entirely by increasing the strength of the inter-particle contact interaction or by implementing a LHY term. The LHY term enables the mean field GPe to describe systems that previously led to a breakdown of the model. The increase in range of possible angles Φ seem to vary with g.

It seems that the external confinement has a part in collapsing the system when close to the region of collapse, both with and without the LHY. A square potential would solve this, but by using larger grids and/or lower the oscillator strength ω the same effect is achieved.

The region of LHY stabilization shows some promise when it comes to creating stable droplets, the aim of our studies. Thus far the droplets have not been confirmed by calculations but further investigation seems likely to yield results, especially with the increase in the stability range of the GPe equation shown in the calculations where the parameters were set to $D = 2, g = 40$. However, more tests are needed before any proper predictions can be made.

Chapter 6 | Outlook

There are several possibilities to expand on this topic. Firstly, a broader and deeper study of the parameter regions for collapse and what factors play a role in this. This in connection with expanded research concerning the LHY terms effect on already stable GPe systems could lead to findings concerning densities and energetics. In this, the implementation of a true quasi-2D LHY term would be of great interest as it was recently suggested by Ref. [26]. This specific LHY term might expand the area of droplet formation. Both a thorough derivation and a computational implementation could be possible extensions of this work.

Secondly, rotation of droplets would be interesting as the rotational properties of quasi 2D systems have been studied at great depth. The stability of droplets, vortex formation in future droplets, rotation of anisotropic systems (such as a strongly dipolar systems), are all possible research areas. The hysteresis behaviour in vortex [27] formation in a one dimensional ring confinement is one known property that might exist in a rotational, self-bound droplet. However, the stability of the droplets is the number one priority among these suggestions but even in case of persisting instability one might imagine a system such as described in Ref [4] where the condensate is confined and one has droplets forming in a crystalline formation. Such a system could be stable even if self-bound rotating droplets are not.

Adding a rotation to the has been done in Ref. [9] where the rotational part is added to the time translation operators kinetic energy and to it's effective potential. This implementation already exist in the code used in this project, as showed in Section 4.1.

Thirdly, these simulations have been conducted in imaginary time. It could be interesting to take the calculations into real time. In real time one can study how a droplet develops as you release it from the trap. A droplet in a strong external confinement might become unstable if one release it to abruptly. The decay of droplets due to three body interactions could also be an interesting topic and only possible to study in real time. To do this, one would start by finding a stationary state for the condensate wave function using the imaginary time method. Using this as the initial condition, one could use the time translation operator shown in Eq. (4.2) to propagate the state in real time. For small time steps and short time periods this would simulate the systems dynamics.

Bibliography

[1] C.J Pethick, H Smith. *Bose-Einstein condensation in Dilute Gases* Cambridge: Cambridge University Press, 2001.

[2] L. Pitaevskii, S. Stringari. *Bose-Einstein Condensation* Oxford: Oxford University Press, 2003.

[3] T. D. Lee, Kerson Huang, and C. N. Yang, "Eigenvalues and Eigenfunctions of a Bose System of Hard Spheres and Its Low-Temperature Properties" *Phys. Rev.* vol 106, 1135, 1957.

[4] H Kadau, M Schmitt, M Wenzel, C Wink, T Maier, I Ferrier-Barbut, T Pfau, "Observing the Rosensweig instability of a quantum ferrofluid" *Nature*, vol 530, pp. 194–197, 2015

[5] H Kadau, M Schmitt, M Wenzel, C Wink, T Maier, I Ferrier-Barbut, T Pfau, "Observing the Rosensweig instability of a quantum ferrofluid" *Nature*, vol 530, pp. 194–197, 2015

[6] G. Semeghini, G. Ferioli, 1 L. Masi, C. Mazzinghi, L. Wolswijk, F. Minardi, M. Modugno, G. Modugno, M. Inguscio M. Fattori, "Self-bound quantum droplets in atomic mixtures", *Phys. Rev. Lett.* vol 120, 235301, 2018

[7] G. Semeghini, G. Ferioli, 1 L. Masi, C. Mazzinghi, L. Wolswijk, F. Minardi, M. Modugno, G. Modugno, M. Inguscio M. Fattori, "Self-bound quantum droplets in atomic mixtures", *Physical review A* vol 86, 063609, 2012

[8] F. Wächtler and L. Santos, "Ground-state properties and elementary excitations of quantum droplets in dipolar Bose-Einstein condensates" *Phys. Rev. A*, vol 94, 043618, 2016

[9] S.A Chin and E Krotscheck, "Fourth-order algorithms for solving the imaginary-time Gross-Pitaevskii equation in a rotating anisotropic trap" *Phys. Rev. E*, vol 72, 036705, 2005

[10] A. Einstein, *Sitzber. Kgl. Preuss. Akad. Wiss.*, vol 3, 1925

[11] M.H. Anderson J. R. Ensher, M. R. Matthews, C. E. Wieman, E. A. Cornell, "Observation of Bose-Einstein Condensation in a Dilute Atomic Vapor" *Science*, vol 269, pp. 198-201 , 1995

[12] J. J. Sakurai, Jim J. Napolitano *Modern Quantum Mechanics*, Second edition, San Fransisco: Addison-Wesley, 2011.

[13] K.B. Davis, M.-O. Mewes, M. R. Andrews, N. J. van Druten, D. S. Durfee, D. M. Kurn, and W. Ketterle "Bose-Einstein Condensation in a Gas of Sodium Atoms" *Phys. Rev. Lett.*, vol 75, pp. 3969-3974, 1995

[14] C. C. Bradley, C. A. Sackett, J. J. Tollett, and R. G. Hulet "Evidence of Bose-Einstein Condensation in an Atomic Gas with Attractive Interactions" *Phys. Rev. Lett.*, vol 75, pp. 1687-1689, 1995

[15] A. Griesmaier, Jörg Werner, Sven Hensler, Jürgen Stuhler, and Tilman Pfau "Bose-Einstein Condensation of Chromium" *Phys. Rev. Lett.*, vol 94, 160401, 2016

[16] M. Lu, N.Q. Burdick, Seo Ho Youn, and B. L. Lev "Strongly Dipolar Bose-Einstein Condensate of Dysprosium" *science*, vol 94, 043618, 2016

[17] D. S. Petrov, G. E. Astrakharchik, "Ultradilute low-dimensional liquids" *Phys. Rev. Lett.* vol 117, 100401, 2016

[18] C. Weiss, M. Block, D. Boers, A. Eckardt, and M. Holthaus "Ground-State Energy of a Weakly Interacting Bose Gas: Calculation Without Regularization" *Z. Naturforsch.*, vol 59a, pp 1-13, 2003

[19] R. N. Bisset and P. B. Blakie, "Crystallization of a dilute atomic dipolar condensate" *Phys. Rev. A*, vol 92, 061603(R), 2015

[20] C. R. Cabrera L. Tanzi, J. Sanz, B. Naylor, P. Thomas, P. Cheiney, and L. Tarruell "Quantum liquid droplets in a mixture of Bose-Einstein condensates" *Science*, vol 359, pp. 301-304, 2018

[21] N. B. Jørgensen, G. M. Bruun, and J. J. Arlt "Dilute Fluid Governed by Quantum Fluctuations" *Phys. Rev. Lett.*, vol 121, 173403, 2018

[22] L. Tanzi, E. Lucioni, F. Famà, J. Catani, A. Fioretti, C. Gabbanini, and G. Modugno "Observation of stable stripes in a dipolar quantum gas" *arXiv:1811.02613*, 2018

[23] J. C. Cremon, G. M. Bruun, and S. M. Reimann, "Tunable Wigner States with Dipolar Atoms and Molecules" *Phys. Rev. Lett.*, vol 105, 255301, 2010

[24] M. Aichinger S.A.Chin E.Krotscheck "Fourth-order algorithms for solving local Schrödinger equations in a strong magnetic field" *Computer Physics Communications*, vol 171, pp. 197-207, 2005

[25] G. M. Brunn, "Bogoliubov transformation and the LHY term", *Notes provided in personal correspondence*, 2018

[26] P. Zin, M. Pylak, T. Wasak, M Gajda and Z Idziaszek "Quantum Bose-Bose droplets at a dimensional crossover" *Phys. Rev. A*, vol 98, 051603, 2018

[27] S Eckel, J.G Lee, F Jendrzejewski, N Murray, C.W Clark, C.J Lobb, W.D Phillips, M Edwards G.K Campbell, "Hysteresis in quantized superfluid 'atomtronic' circuit", *Nature*, vol 506, pp. 200-203, 2014